Spin polarized neutron reflectivity study of a Co/Cu superlattice

A. Schreyer, Th. Zeidler, Ch. Morawe, N. Metoki, and H. Zabel
Experimentalphysik IV, Ruhr-Universität Bochum W-4630 Bochum 1, Germany

J. F. Ankner and C. F. Majkrzak
National Institute of Standards and Technology Gaithersburg, Maryland 20899

(Received 16 November 1992; accepted for publication 9 February 1993)

We present spin polarized neutron reflectivity data on a Co/Cu(111) superlattice and show how not only the magnitude but also the orientation of the average magnetic moment of each layer can be extracted by analyzing the polarization of the reflected beam. This method allows more detailed conclusions about the exchange coupling of magnetic layers across nonmagnetic interlayers and the magnetic in-plane anisotropy in such systems. We present a theoretical fit to the spin-flip and non-spin-flip data which leads to quantitative conclusions about the spin structure. These spin polarized neutron reflectivity results coincide well with the macroscopic magnetic properties which were measured using the magneto-optic Kerr effect revealing a newly discovered uniaxial anisotropy in this system.

I. INTRODUCTION

Recently there has been increasing interest in the magnetic properties of metallic multilayers and superlattices. This interest has been spurred by the discovery of antiferromagnetic exchange coupling between magnetic layers across nonmagnetic spacers and its oscillation between ferro- and antiferromagnetic with increasing spacer thickness.[1] Furthermore, the magnetic anisotropy in such structures and enhanced magnetic moments in very thin films are of current interest.[2] In this paper we present experimental results from spin polarized neutron reflectivity (SPNR) and magneto-optic Kerr effect (MOKE) measurements on the exchange-coupling and the anisotropy of a Co/Cu (111) superlattice and compare the two methods, which are both ideally suited for studies of thin film magnetic structures. We present SPNR data where the polarization state of the incident *and* reflected neutrons has been determined and show that this information can be used to extract the absolute value of the average magnetic moment of each layer as well as its orientation. By doing so we extend an earlier SPNR study by Schwarzacher *et al.* on polycrystalline Co/Cu multilayers.[3] For the first time we show and discuss quantitative fits to all four cross sections of the measured data.

II. NEUTRON REFLECTIVITY CALCULATION

The information contained in spin polarized neutron reflectivity measurements can be quantitatively understood using standard optical methods modified for the effect of the neutron's magnetic moment on the scattering.[4,5] This results from solving the Schrödinger equation for the case of a two component wave function with one component for each of the two possible neutron spin eigenstates + and − in an external magnetic field. A set of two coupled equations results where the interaction potential of the polarized neutrons with the sample is given by the elements of a 2×2 matrix, which are proportional to the effective scattering length density $N^l b^l_{\text{eff}}$. Here N^l is the average atomic density of scatterers and b^l_{eff} the average effective scattering length per atom in layer l of the superlattice. For the typical scattering geometry of a reflectivity measurement with the scattering vector $\mathbf{Q} = (\mathbf{k}_f - \mathbf{k}_i) \| \mathbf{z}$, where $\mathbf{z}$ is defined to be parallel to the sample surface normal, these effective scattering lengths b^l_{eff} (incident polarization, exit polarization) are

$$b^l_{\text{eff}}(\pm,\pm) = (b^l \pm A\mu^l_y), \tag{1}$$

$$b^l_{\text{eff}}(+,-) = b^l_{\text{eff}}(-,+) = A\mu^l_x, \tag{2}$$

with the geometry shown in Fig. 1 , the average nuclear scattering length b^l of the atoms in layer l, the in-plane x- and y-components of the respective average magnetic moment $\boldsymbol{\mu}^l$, a constant $A = 0.2695 \times 10^{-4}$ Å$/\mu_B$ with the Bohr magneton μ_B and the polarization $\mathbf{P}$ of the neutrons defined to be parallel (+) [antiparallel (−)] to the y-axis. $\mathbf{k}_f$ and $\mathbf{k}_i$ are the final and incident wave vectors of the neutrons of wavelength λ with $|\mathbf{k}_f| = |\mathbf{k}_i| = 2\pi/\lambda$. Any component of $\boldsymbol{\mu}^l$ parallel to the surface normal, i.e., $\|\mathbf{Q}$, is not detectable in this scattering geometry.[6] This is generally no problem because in many cases the magnetic moment has no out-of-plane component due to the shape anisotropy in thin films. Nonetheless for very thin films an out-of-plane anisotropy, leading to $\boldsymbol{\mu}^l \| \mathbf{Q}$, may arise.[7] In this case a scattering geometry with an in-plane component of $\mathbf{Q}$, such as grazing incidence Bragg diffraction (GID)[8] could be used. With such a technique all components of $\boldsymbol{\mu}^l$ perpendicular to $\mathbf{Q}_{\text{in-plane}}$ could be mapped out.[9] As discussed further below, it has been confirmed by MOKE that for the present sample the moments are in-plane.

Equation (1) describes the non-spin-flip (NSF) process where the polarization of the neutrons is not altered by the sample. In this case the y-component of the in-plane magnetic moment and the nuclear scattering length both contribute to the reflectivity. On the other hand, the spin-flip (SF) reflectivity is only due to the x-component of the

 0021-8979/93/117616-06$06.00

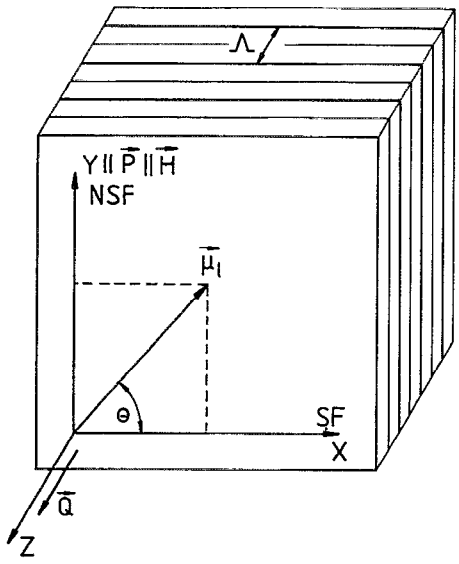

FIG. 1. Schematic view of a superlattice showing the scattering geometry and the sample coordinate system.

in-plane moment, as can be seen from Eq. (2). Therefore the absolute value *and* orientation of the average magnetic in-plane moment for each layer can be determined by extracting the x- and y-components of μ^l from fits of theoretical reflectivities to the NSF and SF data. These reflectivities can be calculated from a dynamical model via the solutions of the Schrödinger equation for the case of a single abrupt interface. Using boundary conditions a matrix formalism for the transmittivity and reflectivity coefficients of a single abrupt interface has been developed.[4,5] To obtain the reflectivity matrix of a superlattice, the appropriate single interface matrices are multiplied. The effect of interface roughness can be modeled by introducing a "smeared out" step profile using the function erf(z) which is then approximated by a number of very thin slabs with abrupt interfaces.[10] The experimental effect of a finite resolution is incorporated by integrating over an incident intensity with a gaussian distribution in $\mathbf{Q}$.

The dynamical formalism described above is exact over the whole $|\mathbf{Q}|$ -range. It accounts for the optical effects of total reflection, refraction and multiple scattering, which are dominant at very low $|\mathbf{Q}|$. Nevertheless it lacks the physical transparency of the simpler kinematical treatment which is valid only far above the regime of total reflection since it does not describe the optical effects listed above. A comparative description of the kinematical as well as the dynamical theory of neutron scattering of superlattices is provided in Ref. 4.

In the case of a superlattice consisting of a number of equivalent bilayers of two materials with a period Λ defined as the bilayer thickness, superlattice peaks separated by $2\pi/\Lambda$ in $|\mathbf{Q}|$ appear as a distinct feature of a reflectivity scan. In a superlattice with one magnetic material per bilayer, antiferromagnetic coupling over the nonmagnetic layer may exist for certain layer thicknesses.[1] This leads to an additional superlattice period of $2 \times \Lambda$ due to the sensitivity of the neutrons to the orientation of the magnetic moments in each layer as shown by Eqs. (1) and (2). As a result, additional half order superlattice peaks of purely magnetic origin appear at positions $|\mathbf{Q}| = \pi/\Lambda$. In a similar fashion magnetic superlattice peaks are obtained for any periodic oscillation of θ, not only for $\Delta\theta = 180°$ and a period of two bilayers as in the case of simple antiferromagnetic coupling. As a consequence, from the quantitative analysis of NSF and SF reflectivity data using the dynamical formalism described above, detailed microscopic information on the spin structure of superlattices can be obtained. In addition, reflectivity measurements are very sensitive to the roughness of the interfaces and to fluctuations of individual layer thicknesses.

Therefore SPNR with polarization analysis can be considered an ideal method for the study of magnetic and structural properties of superlattices hardly surpassed by any other single method in the wealth of information it provides.

III. EXPERIMENTAL METHODS

The Co/Cu (111) superlattice of nominal composition [18 Å Cu/43 Å Co]×6 was grown at room temperature starting with Co on a well polished single crystalline 0.5 in.×1.0 in. $Al_2O_3(11\bar{2}0)$ substrate using sputter procedures described elsewhere.[11] The sample had been thoroughly characterized with x-ray methods[12] confirming good epitaxy of the layers with pure fcc stacking (bulk Co is hcp) and a coherent strain with lattice constants which are consistent with theory using bulk elasticity models. The out-of-plane mosaicity was determined to be less than 0.02°. The nominal sample composition has been confirmed with an accuracy of a few percent by combining the result of a chemical analysis using x-ray fluorescence with the bilayer thickness measured with x-ray reflectivity.

The SPNR measurements were performed at the Research Reactor of the National Institute of Standards and Technology in Gaithersburg/USA on the reflectometer BT-7.[4] Using an Fe/Si supermirror, a monochromated neutron beam of the wavelength 2.367 Å was polarized, reflected by the sample and then polarization-analyzed by an identical Fe/Si supermirror. Two spin flippers mounted in front of and behind the sample, respectively, were used to measure all four cross sections $R(+,+)$, $R(-,-)$,$R(-,+)$ and $R(+,-)$, where $+(-)$ is the neutron spin state parallel (antiparallel) to a field $\mathbf{H}$ applied in the sample surface plane, normal to the scattering vector $\mathbf{Q}$. This neutron guide field is parallel to the y-axis defined above and was chosen to be 1.4 mT which is small enough not to destroy any possible antiferromagnetic order in the sample. Prior to the measurements, the sample had been saturated in a field of 20 mT parallel to the y-axis. The reflectivity scans were taken by varying $\mathbf{Q}$ in a standard $\Theta/2\Theta$ mode. The diffuse scattering beneath the specular ridge has been characterized separately by a $(\Theta + \delta\Theta)/2\Theta$-scan with a small offset $\delta\Theta$ and subtracted from the measured specular intensity. The data have also been corrected for the geometrical effect of the finite sample size.

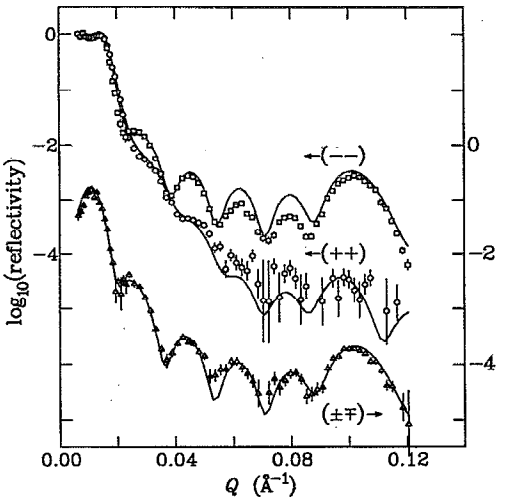

FIG. 2. Four cross section reflectivity scan of the sputtered Co/Cu(111) superlattice with a fit to the data. The SF reflectivities have been added and are shifted downwards by two orders of magnitude.

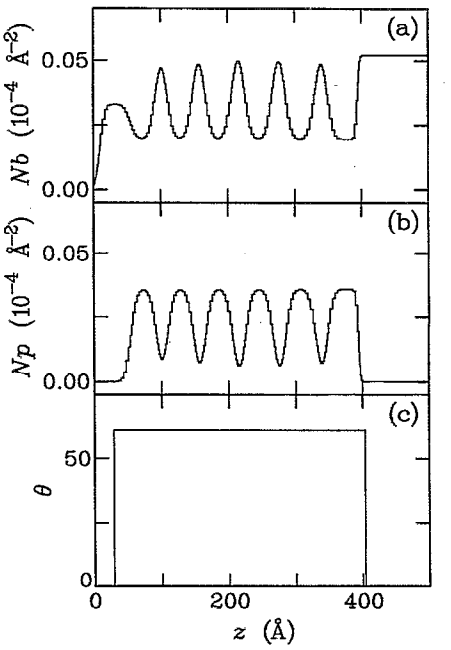

FIG. 3. Nuclear (a) and magnetic (b) scattering length density profiles as well as the θ-profile (c) for the fitted reflectivities shown in Fig 2.

As opposed to the microscopic spin structure determined by SPNR, MOKE is well suited for the analysis of the macroscopic magnetic properties of thin film systems.[13] Using the proportionality between the Kerr angle and the sample magnetization, hysteresis curves can be obtained by measuring the rotation of the Kerr angle as a function of an applied field. From the form of these curves, information on anisotropies and the microscopic spin structure can be inferred. Nonetheless, this macroscopic method cannot provide direct proof of microscopic spin structures and coherence lengths. By combining SPNR and MOKE, one can construct a detailed picture of the magnetic properties of a multilayer film.

The MOKE was measured using a lock-in modulation technique providing a resolution of $< 5 \times 10^{-4}$ deg and employing the longitudinal geometry, with the external field parallel to the film planes. The samples were rotated around an axis perpendicular to the film planes by a few degrees between subsequent measurements to obtain information about the in-plane anisotropy from the hysteresis curves.[14] In addition, the polar geometry with the field perpendicular to the film plane was used to confirm that the magnetic moments had no out-of-plane component.

IV. EXPERIMENTAL RESULTS

In Fig. 2 the SPNR data of the superlattice are shown together with a fit. The two SF cross sections have been added to improve statistics since they were measured to be equal, as expected from Eq. (2). At very low $\mathbf{Q}$, the regime of total reflection can be seen in the NSF data up to the critical angle of total reflection $\mathbf{Q}_C^{\mathrm{NSF}}$ whereas the SF data shows a more complicated structure, which will be discussed further below. The first superlattice peak, at about $|\mathbf{Q}| = 0.1$ Å^{-1}, can easily be identified in the $(-,-)$ and the SF data. The absence of the peak in the $(+,+)$ data is due to the fact that the effective scattering length densities of Co and Cu are approximately equal for this neutron polarization, leading to a very low scattering contrast between the two materials. The four oscillations between the superlattice peak and $\mathbf{Q}_C^{\mathrm{NSF}}$ are the $n-2$ secondary maxima of this superlattice with $n=6$ Co/Cu double layers.[15] The distance $|\Delta\mathbf{Q}|$ between these maxima is related to the overall thickness D of the superlattice via $|\Delta\mathbf{Q}| = 2\pi/D$. Although antiferromagnetic interlayer coupling would have been expected for the Cu thicknesses of this sample, no sign of a half order peak around $|\mathbf{Q}| = 0.05$ Å^{-1} is visible. Furthermore, keeping in mind that the SF data only contains magnetic information, its close similarity to the NSF data unambiguously proves that the nuclear and magnetic periodicities and the respective coherence lengths in this sample are identical.

The strong SF reflectivity, which is observed despite the initial saturation of the sample along the y-axis, is a consequence of a strong in-plane anisotropy. This causes the Co moments to align along an easy axis, which must be tilted away from the y-axis, leading to a large x-component of the $\boldsymbol{\mu}'$.

These qualitative conclusions are quantitatively confirmed by the simultaneous fit to all four cross sections of the data which is shown in Fig. 2. Employing the dynamical formalism described above, the fitted reflectivities were calculated from the nuclear and magnetic scattering length density profiles shown in Figs. 3(a) and 3(b), respectively, with the in-plane orientation of the Co moments being constant at $\theta = 60°$ over the whole sample thickness range [Fig. 3(c)]. Here polar coordinates with the magnetic scattering length $p = A|\boldsymbol{\mu}|$ have been used (see Fig. 1). The average magnetic moment of the Co was found to be 1.7 μ_B, consistent with its bulk value and the rms Gaussian roughness $\sigma = \sqrt{\langle z \rangle^2}$ at the Co/Cu interfaces was 7.1 Å.

TABLE I. Fitted parameters from SPNR data. From left-to-right these are: layer number l (layer 0 is incident air); a brief description of the layer; real part of the average nuclear scattering density Re(Nb); nuclear layer thickness d_b; nuclear Gaussian mixing σ_b; magnetic scattering density Re(Np); magnetic layer thickness d_p; magnetic Gaussian mixing σ_p; and the angle of the magnetic moment with respect to the spin-flip (incident beam) direction.

l	Type	Re(Nb) (10^{-6} Å^{-2})	d_b (Å)	σ_b (Å)	Re(Np) (10^{-6} Å^{-2})	d_p (Å)	σ_p (Å)	θ (deg)
1	CuO_x	3.3	45.0	5.8	0	45.0	5.8	0
2, 4,...,12	Co	2.0	41.1±3.3	7.1	3.6	41.1±3.3	7.1	60
3, 5,...,11	Cu	5.6	18.6±1.2	7.1	0	18.6±1.2	7.1	0
13	Al_2O_3	5.2	...	2.1	0	...	2.1	0

By including a fluctuation of the individual layer thicknesses of up to ±8% the observed intensity of the finite thickness oscillations was better reproduced by the fit. Finally a reduction of the average atomic density N^l of each layer by about 13% resulted, leading to a minimized χ^2 (as defined, e.g., in Ref. 10) of 17.6. A reduction of N^l has also been found by Schwarzacher *et al.*[3] for their Co/Cu multilayers. The fit parameters are summarized in Table I.

As a consequence of the rather large roughness in this specific sample, the magnetic scattering length density does not become zero in the Cu layers in this model [see Fig. 3 (b)]. Therefore we cannot exclude the existence of pinholes which might explain the absence of antiferromagnetic coupling in this sample. On the other hand we find sharp interfaces, no sign of pinholes and a waviness on the order of 100 Å from transmission electron microscopy of a similarly sputtered polycrystalline Co/Cu multilayer on a glass substrate.[16] This discrepancy could be explained by the fact that specular reflectivity cannot distinguish between waviness and interface roughness. Off specular measurements will shed more light on this problem in the near future.

The fit also very nicely reproduces the first peak at $\mathbf{Q}_P^{SF}$ at $|\mathbf{Q}| \approx 0.01$ Å^{-1} in the SF-data and the corresponding small dip in the NSF data below $\mathbf{Q}_C^{NSF}$. This dip is a direct consequence of the law of particle conservation since, in the regime of total external reflection, the NSF intensity has to be reduced to account for any nonzero SF intensity. To be able to understand the nature of this SF peak it must be noted that, even in the regime of total reflection, any quantum mechanical particle has a nonnegligible penetration depth resulting from tunneling.[8] This penetration depth is a sensitive function of $\mathbf{Q}$ and leads to an interaction of the incident polarized neutrons with the sample's magnetic moments also in the regime of "total" external reflection. The existence of the SF peak at $\mathbf{Q} = \mathbf{Q}_P^{SF}$ can be understood by correlating the optical path length of the neutrons inside the sample with $\mathbf{Q}$. For $\mathbf{Q} = \mathbf{Q}_P^{SF}$ the path length of the neutrons in the magnetic parts of the sample allows a maximum number of neutrons to pick up the energy needed to flip their polarization state.

From experiments and theoretical simulations we find that the intensity of the peak at $\mathbf{Q}_P^{SF}$ is a sensitive function of the in-plane orientation of the magnetic moments, as would be expected from Eq. (2). In the case of $\theta=0°$ all incident neutrons are flipped into their opposite states leading to a SF reflectivity of 100% for $\mathbf{Q} = \mathbf{Q}_P^{SF}$, whereas the NSF intensity is zero at this $\mathbf{Q}$. The SF intensity goes down rapidly with increasing θ and becomes zero for $\theta = 90°$ consistent with Eq. (2). Consequently the NSF intensity increases and shows a plateau without a dip for $\theta=90°$ in the regime of total reflection.

Therefore not only the data above $\mathbf{Q}_C^{NSF}$ but also the data in the regime of total reflection are very sensitive to details of the magnetic structure of the sample. This finding may lead to new applications in the future, since below $\mathbf{Q}_C^{NSF}$ the reflected intensity is at its maximum, allowing a reduced counting time.

In our model we have assumed the presence of only one magnetic domain. This assumption can be checked directly by comparing SPNR scans for different sample orientations with theory. This can be done, e.g., with the magnetic moments aligned along the x- and y-axes, respectively, as described above. Nevertheless, the MOKE hysteresis curves also render information on the presence of domains in the sample.

The MOKE measurements in the polar geometry show typical hard axis hysteresis curves which confirm that the magnetic moments have no out of plane component. This agrees with the neutron result of an in-plane magnetic moment with the magnitude of bulk Co. In Fig. 4 , two hysteresis curves measured in the longitudinal geometry are shown for different turn angles θ', as defined in the inset. The square hysteresis loop of Fig. 4(a) is typical for an easy axis whereas the loop shown in Fig. 4(b) for the sample turned by 90° corresponds to a hard axis. The form of the loops oscillates between the two extrema of Figs. 4(a) and 4(b) as a function of the turn angle with an easy axis loop at $\theta'_{\text{easy }1} = 60°$ and $\theta'_{\text{easy }2} = \theta'_{\text{easy }1} + 180°$. The hard axis loops appear at $\theta'_{\text{easy }1} + 90°$ and $\theta'_{\text{easy }1} + 270°$. These facts imply that the easy axis is tilted away from the x-axis by $\theta'_{\text{easy}} = 60°$ and that the anisotropy is uniaxial. This is a surprising result since only a weak sixfold anisotropy would have been expected for the (111) plane. Nonetheless for a certain range of overall thicknesses D this uniaxial magnetic anisotropy is a common feature of all our sputtered Co/Cu(111) superlattices which have been grown on $Al_2O_3(11\bar{2}0)$ substrates. Furthermore it coincides perfectly with the in-plane spin orientation of $\theta=60°$ determined with SPNR using exit beam polarization analysis.

The form of the easy axis MOKE hysteresis curve of Fig. 4(a) confirms our SPNR result of the presence of only

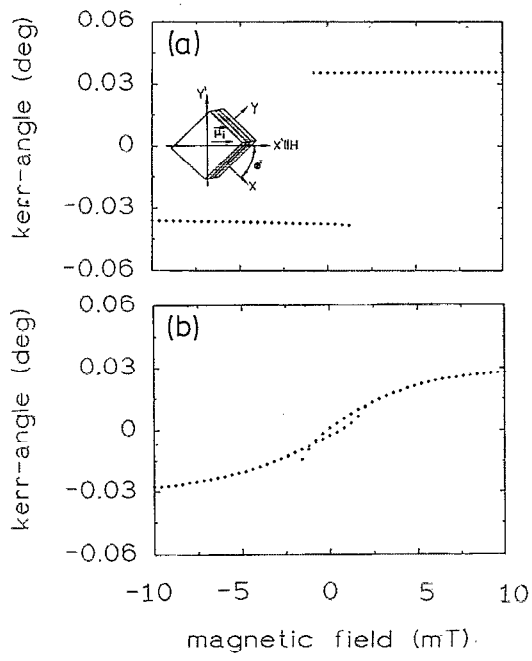

FIG. 4. MOKE hysteresis curves for $\theta' = 60°$ (a) and $\theta' = 150°$ (b). The primed laboratory reference frame and the sample turn angle θ' are defined by the inset. The magnetic field is parallel to the x'-axis.

one magnetic domain in the sample. The strong uniaxial anisotropy seems to prevent domain formation, leading to the observed square form of the hysteresis curve. In the case of domain formation the remanent magnetization should be smaller than the saturation magnetization.

A uniaxial anisotropy of thin hcp Co(0001) films on $Al_2O_3(11\bar{2}0)$ has been observed for the first time by Metoki *et al.*[14] They found it to be a pure interface effect and propose that it may be due to a partial internal oxidation of Co atoms at the interface by the topmost oxygen atoms of the Al_2O_3, which appear to be lined up with the hard axis of the Co. Using the same x-ray GID techniques as in Ref. 14 one finds the same orientational relation between the hard axis and the Al_2O_3 in the superlattice sample discussed here. A lattice distortion with a twofold symmetry which might cause this effect was detected neither in the case of the single Co films nor for the present Co/Cu(111) superlattice. The behavior of $Co/Al_2O_3(11\bar{2}0)$ is in marked contrast to the observation of a uniaxial anisotropy for ultrathin Co films on Cu substrates,[17] which is induced by steps on the surface of the substrate. For $Co/Al_2O_3(11\bar{2}0)$, no correlation between the observed uniaxial anisotropy and steps on the sapphire was observed.

As shown by SPNR, MOKE and GID a uniaxial magnetic anisotropy of presumably the same origin as in the $Co/Al_2O_3(11\bar{2}0)$ films exists in the Co/Cu(111) superlattice studied here, leading to a parallel orientation of the magnetic moments in all layers with $\theta = 60°$. Further work clarifying the dependence of the strength of the anisotropy on the overall thickness D and the individual layer thicknesses will shed more light on the nature of this magnetic anisotropy.

V. CONCLUSIONS

We have shown how SPNR with exit beam polarization analysis can be used to determine the magnitude *and* orientation of the in-plane average magnetic moment in a superlattice. We are able to model the data in detail using a fitting routine which allows the quantitative determination of the interface roughnesses, individual layer thicknesses and the orientation of the magnetic moment. Despite an initial magnetization of the sample along the y-axis we find that all spins in the Co layers are tilted away from this magnetization axis. These SPNR results are in very good agreement with MOKE data, revealing a newly discovered unusual uniaxial magnetic anisotropy in this system. Further work on superlattices with oscillatory exchange coupling showing spin structures which deviate from simple parallel or antiparallel alignment is in progress.

ACKNOWLEDGMENTS

This work has been supported in part by the Deutsche Forschungsgemeinschaft through SFB 166. Furthermore we gratefully acknowledge the travel support received from NATO through CRG 901064.

[1] C. F. Majkrzak, J. W. Cable, J. Kwo, M. Hong, D. B. McWhan, Y. Yafet, J. V. Waszczak, and C. Vettier, Phys. Rev. Lett. **56**, 2700 (1986); P. Grünberg, R. Schreiber, Y. Pang, M. B. Brodsky, and H. Sowers, *ibid.* **57**, 2442 (1986); S. S. P. Parkin, R. Bhadra, and K.P. Roche, *ibid.* **66**, 2152 (1991).

[2] E.g., G. P. Felcher, K.E. Gray, R.T. Kampwirth, and M. B. Brodsky, Physica B&C **136**, 59 (1986); J. A. C. Bland, D. Pescia, and R. F. Willis, Phys. Rev. Lett. **58**, 1244 (1987); Y. Y. Huang, C. Liu, and G. P. Felcher, Phys. Rev. B **47**, 183 (1993).

[3] W. Schwarzacher, W. Allison, J. Penfold, C. Shackleton, C. D. England, W. R. Bennet, J. R. Dutcher, and C. M. Falco, J. Appl. Phys. **69**, 4040 (1991).

[4] C. F. Majkrzak, Physica B **173**, 75 (1991).

[5] C. F. Majkrzak, to appear in *Handbook of Neutrons*, edited by W. Gläser (Springer, Berlin) (in press); S. J. Blundell and J. A. C. Bland, Phys. Rev. B **46**, 3391 (1992); G. P. Felcher, R. O. Hilleke, R. K. Crawford, J. Haumann, R. Kleb, and G. Ostrowski, Rev. Sci. Instrum. **58**, 609 (1987); S. K. Mendiratta and M. Blume, Phys. Rev. B **14**, 144 (1976); V. A. Belyakov and R. Ch. Bokun, Fiz. Tverd. Tela (Leningrad) **18**, 2399 (1976) [Sov. Phys. Solid State **18**, 1399 (1976)]; P. J. Sivardiere, Acta Crystallogr. A **31**, 340 (1975).

[6] E.g., V. F. Sears, *Neutron Optics* (Oxford University, Oxford, 1989), p. 89.

[7] L. Néel, J. Phys. Rad. **15**, 225 (1954).

[8] This technique is routinely used with x rays and has recently also been demonstrated for neutrons: see J. F. Ankner, H. Zabel, D. A. Neumann, and C. F. Majkrzak, Phys. Rev. B **40**, 792 (1989); K. Al Usta, H. Dosch, A. Lied, and J. Peisl, in *Surface X-Ray and Neutron Scattering*, edited by H. Zabel and I. K. Robinson, Springer Proceedings in Physics (Springer, Berlin, 1992), Vol. 61, p. 239.

[9] J. F. Ankner, C. F. Majkrzak, D. A. Neumann, A. Matheny, and C. P. Flynn, Physica B **173**, 89 (1991).

[10] J. F. Ankner and C. F. Majkrzak, in *Neutron Optical Devices and Applications*, SPIE Conference Proceedings, Vol. 1738 (SPIE, Bellingham, WA) (in press); J. F. Ankner, in *Surface X-Ray and Neutron Scattering*, edited by H. Zabel and I. K. Robinson, Springer Proceedings in Physics, (Springer, Berlin, 1992), Vol. 61, p. 105.

[11] Ch. Morawe, A. Stierle, N. Metoki, and H. Zabel, J. Magn. Magn. Mater. **102**, 223 (1991).

[12] P. Bödeker, A. Abromeit, K. Bröhl, P. Sonntag, N. Metoki, and H. Zabel, Phys. Rev. B **47**, 2353 (1993).

[13] S. D. Bader, J. Magn Magn. Mater. **100**, 440 (1991).

[14] N. Metoki, Th. Zeidler, A. Stierle, K. Bröhl, and H. Zabel, J. Magn. Magn. Mater. **118**, 57 (1993).
[15] F. Rieutord, J. J. Benattar, R. Rivoira, Y. Lepêtre, C. Blot, and D. Luzet, Acta Crystallogr. A **45**, 445 (1989).
[16] Ch. Morawe, A. Abromeit, M. Hofelich, N. Metoki, U. Romahn, A. Schreyer, P. Sonntag, Th. Zeidler, H. Zabel, J. F. Ankner, and C. F. Majkrzak (unpublished).
[17] A. Berger and H.P. Oepen, Phys. Rev. Lett. **68**, 839 (1992).